JOURNAL OF MATERIALS SCIENCE 29 (1994) 1884–1894

Characterization of (Pb, La) TiO_3 thin films prepared by the sol–gel method

JANG-CHENG HO, I-NAN LIN*, KUO-SHUNG LIU
*Department of Materials Science and Engineering, and *Materials Science Center, National Tsing-Hua University, Hsinchu 30043, Taiwan*

$Pb_{(1-1.5x)}La_xTiO_3$ thin films were synthesized by the sol–gel spin-coating technique. The films became crystallized when the spin-coated films were annealed at 600 °C and at higher temperature, and became amorphous when annealed at 550 °C. The breakdown voltage, V_B, was recorded at around 30 V for 600–650 °C annealed films and varied only slightly with the composition. The V_B value of the amorphous films was observed to be higher than that of the crystalline films. The ferroelectric properties of both the amorphous and crystalline films were found to be similar. The dielectric constant, charge storage density and optical index of refraction of the films were $\varepsilon_r = 5$–20, $Q_c = 0.12$–0.54 μC cm^{-2} and $n = 1.6$–2.3, respectively. They all increased moderately with La^{3+} content in the films. One possible reason why the ferroelectric properties are not modified as the amorphous films crystallize, may be that the octahedra are equilateral, whether the films are amorphous or crystalline. Additionally, a possible cause which lowers the breakdown voltage in crystalline film, is the formation of lead vacancies due to lead loss. The electrical properties of films coated on bare silicon become significantly lowered due to interdiffusion between films and substrate. The diffusion of Si^{4+} ions into the films can be prevented by coating $SrTiO_3$ on the silicon substrate as a buffer layer. The charge storage capacity consequently becomes substantially enhanced.

1. Introduction

Lead titanate (PT) possesses the most remarkable ferroelectric, pyroelectric and piezoelectric properties of the perovskite materials, owing to its large tetragonality ($c/a = 1.06$), and high Curie temperature ($T_c = 490$ °C). The requirements of low operating voltage and large component area have increasingly been considered in the light of recent critical device application, e.g. non-volatile memories and pyroelectric detectors. PT films have, therefore, attracted a substantial amount of attention and have been synthesized using the r.f.-sputtering technique [1, 2]. Control of the composition of the films is, however, difficult as a result of an unpredictable sputtering cross-section for each species. A variety of wet-chemical deposition methods, including metallo-organic decomposition (MOD) [3, 4] and sol–gel processing [5–10] have thus been investigated and $PbTiO_3$ or lanthanum-doped $PbTiO_3$ thin films have been successfully prepared. Both techniques offer close control of chemical composition and uniform incorporation of minor amounts of dopant. The MOD method requires stringent control of the processing environment as a consequence of a high susceptibility of metallo-organics to hydrolysis. The preparation of precursors in the sol–gel route is, on the other hand, difficult because the solubility of lanthanum acetate becomes limited in the presence of lead acetate [5].

The purpose of this study was to improve the PLT films synthesized via the sol–gel method. The correct combination of raw materials and solvents necessary to circumvent the difficulties which arise from the hydrolysis and solubility of the materials was investigated. The characteristics of PLT films subsequently prepared may be evaluated for their potential use as an MOS (metal–oxide–semiconductor) device.

2. Experimental procedure

The precursors of composition $Pb_{(1-1.5x)}La_xTiO_3$, $x = 0$–0.3, were prepared from lead acetate, lanthanum acetate and titanium isoproxide using glacial acetic acid and 2-methoxyethanol as solvents, and similarly following the method previously developed by Budd *et al.* [5]. The samples are hereafter referred to by their mol % La content (i.e. $Pb_{0.85}La_{0.1}O_3$ is abbreviated to PLT10). The lead acetate and lanthanum acetate powders of correct molar ratio were first mixed and heated in a vacuum at 110 °C for 2 h in order to remove the hydrated water. Excess 5 mol % Pb $(OAc)_2$ was included to compensate for the PbO loss which occurred during the heat-treatment process. The mixture was then dissolved in glacial acetic acid. For each 1 g acetate powder mixture, 2 ml solvent were used. The required amount of titanium isopropoxide was separately dissolved in 2-methoxyethanol and then mixed with the acetate solution. Finally, acetylacetone, equimolar to the cations, was added to stabilize the solution with a PLT precursor (0.5 M) consequently being obtained. All the procedures were carried out under a dry nitrogen atmosphere to prevent hydrolysis of the precursors. The stock

0022–2461

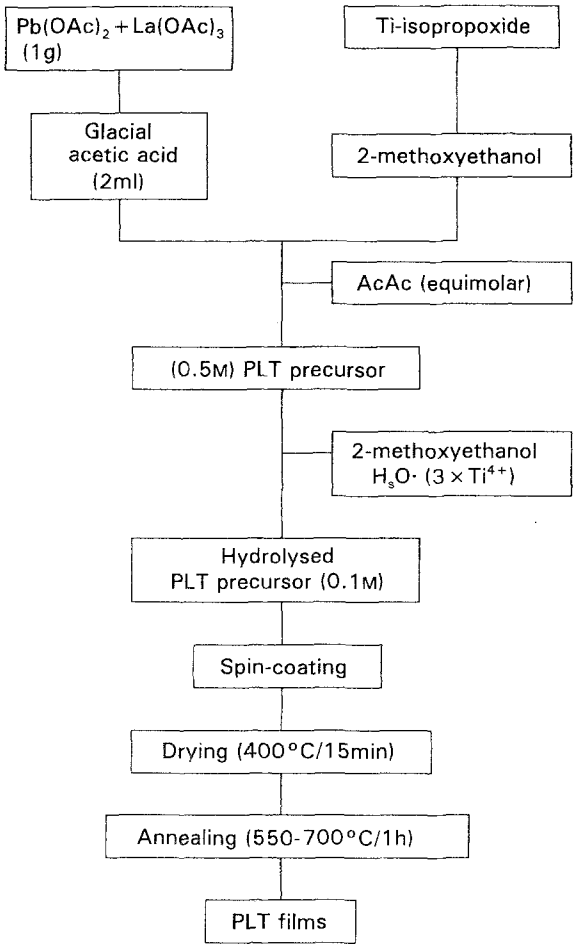

Figure 1 Flow diagram for synthesizing the PLT series of thin films.

solution was diluted to 0.2 M with 2-methoxyethanol prior to synthesizing the films by spin-coating. A small proportion of water, $H_2O:Ti^{4+} = 3:1$, was included in 2-methoxyethanol to control the hydrolysis of the precursors.

For preparation of the PLT using the spin-coating technique, p-type silicon wafers were first cleaned by rinsing in TCE, ACE, and deionized water, which was followed by 1 min etching in 2% HF water solution for removal of the surface oxide. The pre-hydrolysed precursors were next spin-coated on the silicon substrate and dried at 400 °C for 15 min. Five layers of precursors were coated in each film. The dried films were annealed in an oxygen atmosphere at 550–700 °C for 1 h to convert the organic precursors into oxide films. The processing scheme for the synthesis of PLT films is illustrated in Fig. 1. In addition to spin coating on the bare silicon substrate, the PLT films were also prepared using $SrTiO_3$-coated silicon as substrate.

The crystal structure and microstructure of the films were examined using X-ray diffractometry (Rigaku) and scanning electron microscopy (SEM, Joel 840A), respectively. Depth profiles were obtained using secondary ion mass spectrometry (SIMS). The gold electrodes, 0.4 mm diameter, were then fabricated on top of the PLT films by d.c. sputtering through a shadow mask. The current–voltage (I–V) characteristics and capacitance-voltage (C–V) properties of the films were measured using an H.P.4145B parameter analyzer and H.P.4194A impedance analyser, respectively. The charge storage capacities, Q_c, of the films were estimated from the switching characteristics of an RC circuit with 3.3 kΩ load by applying a 5 V step voltage towards the films.

3. Results

3.1. Material characteristics

The decomposition characteristics of the PLT series of precursors are represented as TGA/DTA curves in Fig. 2 which reveal that two exothermic reactions have occurred. The sharp exotherm which occurred at ~ 295 °C is a result of the decomposition of residual organics. The second exothermic reaction reveals the crystallization of the gel. Double reactions are observed for the second process, as indicated by the DTA curves in Fig. 2a–c. These double reactions have first crystallized into a distorted cubic phase at ~ 440 °C and then become transformed into cubic phase at ~ 460 °C [11], but both were characterized by octahedral TiO_6 groups. This phenomenon is not so obvious above a lanthanum content of 5 mol %, owing to decreasing tetragonality. No other reaction is observable for a temperature higher than 500 °C. The results infer that the heat treatment for converting the spin-coated metal–organic films to oxide films should be performed at a temperature higher than this temperature. On the other hand, the potential problem of lead loss which has occurred for all these lead-containing oxides, limits the highest temperature for heat treatment of spin-coated films.

The evolution of the crystal structure of the films at 550–750 °C is examined by the X-ray diffraction method and the results are shown in Fig. 3. The crystallization of films annealed at 550 °C is indicated from this figure to remain incomplete (Fig. 3a). The polycrystalline form of perovskite structure is indicated in Fig. 3b–d to be obtained only for those films annealed at 600 °C and above. The second phase appeared when the low lanthanum-containing films are heat treated at 700 °C. 600–650 °C is inferred from these results to be the most suitable annealing temperature for converting the spin-coated films to perovskite structure.

The films containing no La^{3+} ions, i.e. PT films, are of tetragonal crystal structure, and those films with a lanthanum content higher than 10 mol % are of cubic crystal structure. The morphotropic phase boundary (MPB) composition appears to be the PLT5, which contains 5 mol % lanthanum and is significantly different from that in ceramics form. The MPB of the latter is indicated, from the X-ray patterns provided in Fig. 3g, to be situated between 25 and 30 mol % lanthanum. The Curie temperature for polycrystalline ceramics to transform from cubic to tetragonal is 490 °C for $PbTiO_3$ materials, and is known to decrease as the lanthanum content in $Pb_{(1-1.5x)}La_xTiO_3$ increases. The Curie point of PLT-series films apparently becomes further lowered.

The suppression of cubic to tetragonal transformation has been observed for ultrafine $BaTiO_3$ ceramic materials and has been ascribed to the constraint of the surface tension of the ultrafine grains. The same mechanism is certainly capable of being

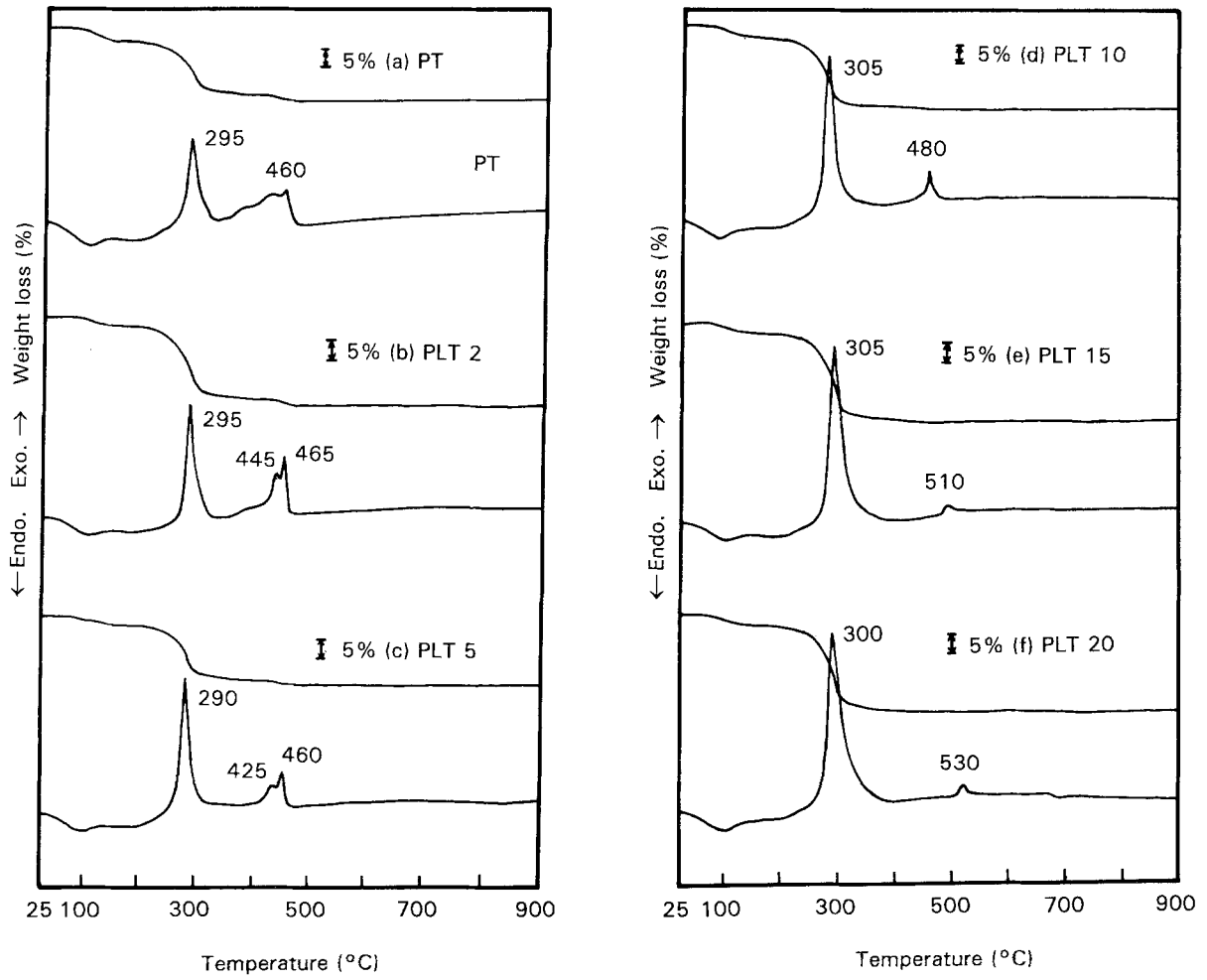

Figure 2 Decomposition characteristics of a gel of (a) $PbTiO_3$, (b) PLT 2, (c) PLT 5, (d) PLT 10, (e) PLT 15, (f) PLT 20, analysed using TGA/DTA (heating rate 5 °C min^{-1}).

applied to the suppression of cubic to tetragonal transformation which occurs in those PLT films, because the crystal size of these films is indicated, from the micrographs provided in Fig. 4, to be of the order of 0.1 μm. However, other constraints arise which should be taken into consideration. The thickness of the films is indicated from Fig. 4a–c to be around 0.3 μm, such that the films contain only one layer of grains. The strain imposed by the substrate is therefore not negligible.

The micrographs of the films were examined using scanning electron microscopy (SEM) and are illustrated in Fig. 5. The films consist of ultrafine grains (~ 0.1 μm) which are observed in Fig. 5a–c to be uniformly distributed all over the surface of PT, PLT5 and PLT10 films. Circular geometric regions with a

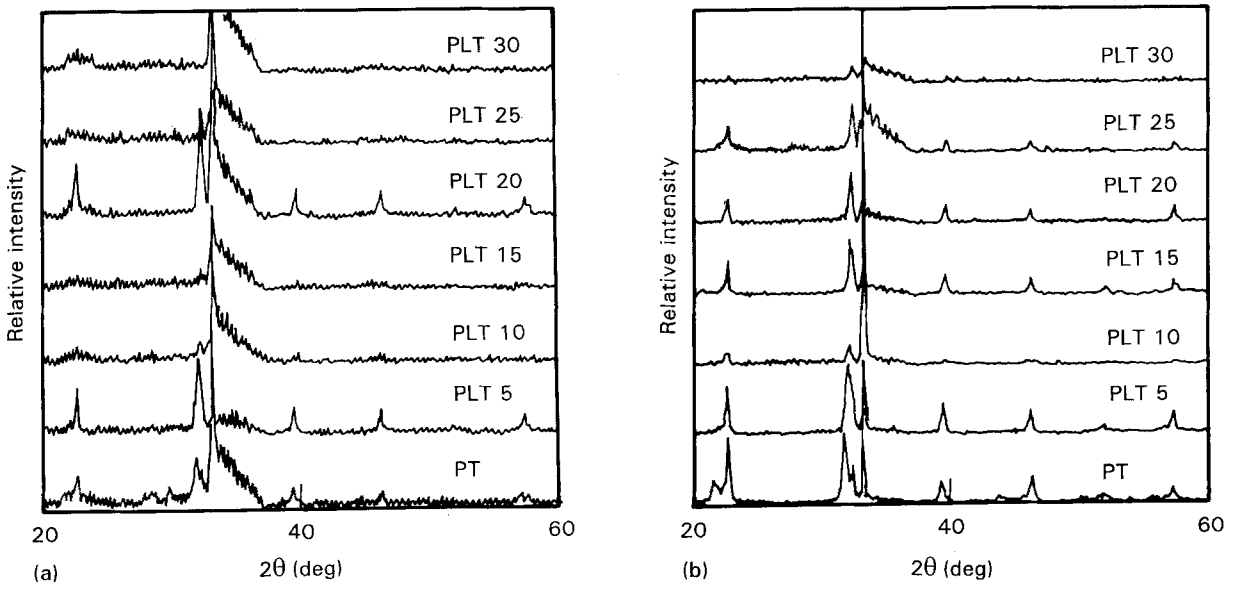

Figure. 3a and b

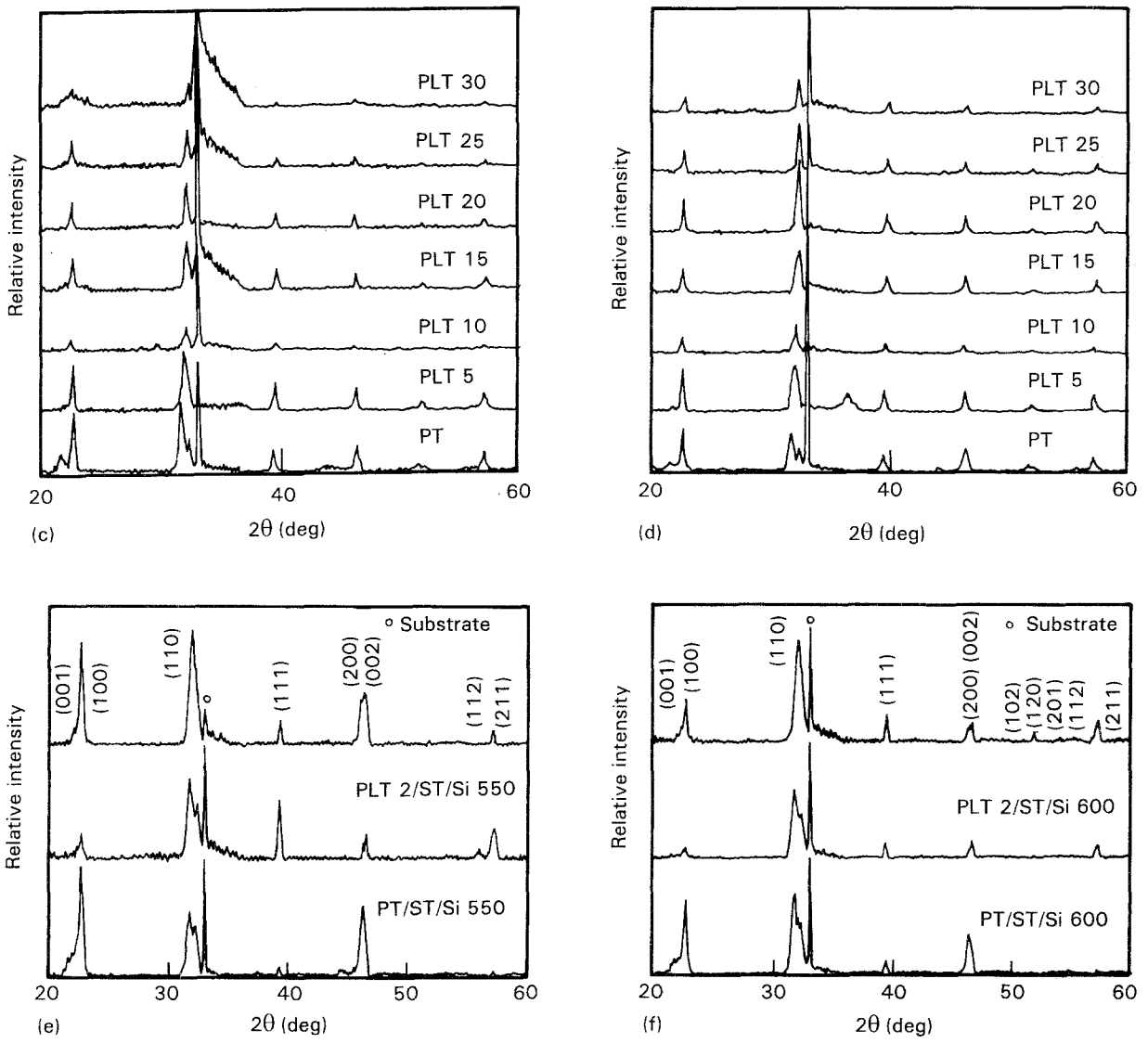

Figure 3 X-ray diffraction of PLT films annealed at (a) 550 °C, (b) 600 °C, (c) 650 °C, (d) 700 °C, coated on bare silicon, annealed at (e) 550 °C, (f) 600 °C coated on $SrTiO_3$ (Si), and that of (g) polycrystalline ceramics.

smooth surface are observed in Fig. 5e and f for films containing more than 20 mol % La. The film PLT15 consists of an ultrafine grain microstructure which is distributed among the large circular regions (Fig. 5d).

3.2. Electrical properties

The leakage current density and charge storage capacities of the PLT films were measured using an H.P.4145B parametric analyser and an H.P.4194A impedance analyser, respectively. All the films are indicated from Fig. 6a–d to possess current–voltage characteristics which are similar to that of varistors; that is, the leakage current density is low at a small applied voltage and abruptly increases once the applied voltage has exceeded certain limits. The variation of breakdown voltage V_B, with composition is narrower for those films annealed at 600–650 °C (Fig. 6b and c). The value of V_B is observed from Fig. 6d to have a scattered distribution for those films annealed at 700 °C (Fig. 6d). This phenomenon possibly occurs as a result of side effects, such as lead loss or second-phase formation, which occurred at a too high temperature applied for heat treatment.

Annealing at 550 °C is indicated from Fig. 6a to result in a breakdown voltage which is significantly higher than in those films which were annealed at 600–650 °C. The films annealed at 550 °C are observed

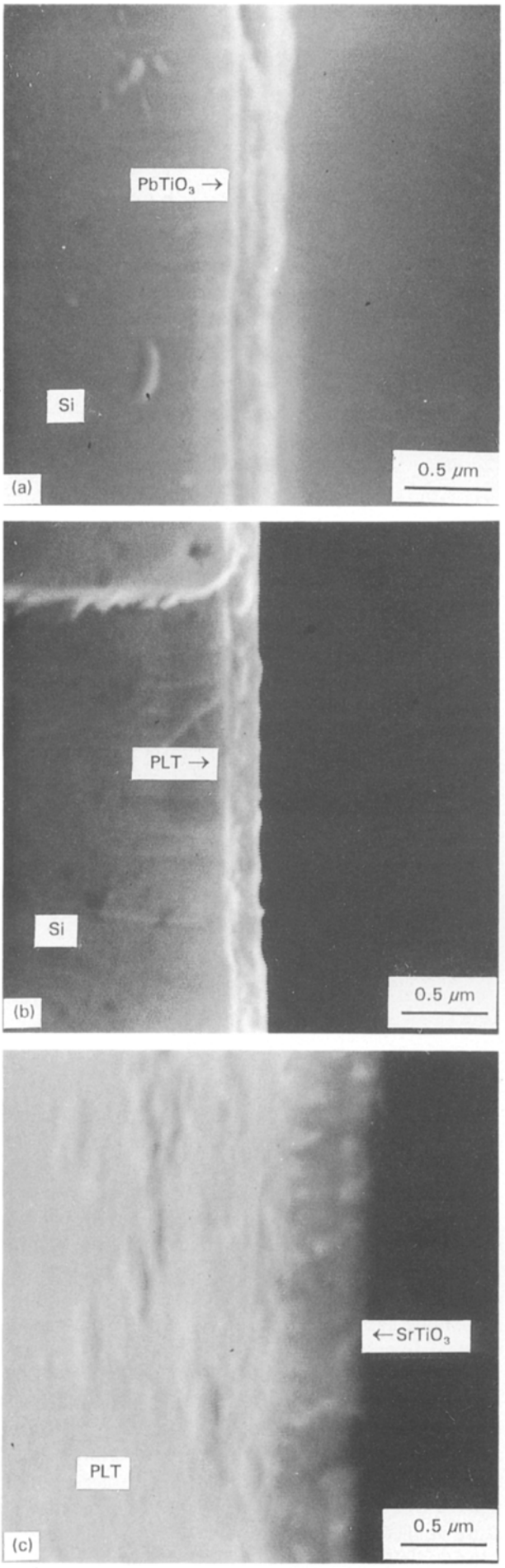

Figure 4 Cross-sectional view of 600 °C annealed films of (a) $PbTiO_3$, (b) PLT 25 coated on silicon, and (c) PLT 10 on $SrTiO_3$ coated silicon.

in Fig. 3a–c to be either amorphous or incompletely crystallized, while those films annealed at 600–650 °C are of a single-phase polycrystalline form. The amorphous form can therefore be concluded to withstand a higher applied voltage and possess a lower leakage current than the crystalline form does.

The C–V curve shown in Fig. 7a represents typical characteristics of the PLT films. The capacitance value becomes large once the metal–oxide–semiconductor configuration of the samples is forwardly biased, and becomes small again once the samples are reversely biased. The dielectric constant of the PLT films has been calculated from the forwardly biased capacitance value for each of the films and is plotted in Fig. 7b. The relationship between heat-treatment temperature and electrical property of the films has no significant correlation with each other. However, the trend by which the dielectric constant of the PLT films increases slowly with La^{3+} concentration, is conceived.

The charge storage capacity of the PLT films was evaluated using the circuit shown in the insert of Fig. 8, where a charging signal was sensed across the resistance in response to the step signal applied across the thin film samples (C) and the resistance (R) connected in series. The charging curves were numerically integrated to estimate the total charge stored in the samples. The variation of charge storage capacity of the films with the composition and annealing conditions is plotted in Fig. 8. The correlation between Q_c and heat-treatment temperature is, again, confirmed from this figure to be insufficiently adequate. However, the increase in charge storage density with La^{3+} content would still be conceivable. These results are consistent with the concentration dependence of dielectric constant shown in Fig. 7b.

The index of refraction of the films was measured using an ellipsometer. These results, again, increased with the proportion of La^{3+} ions in the PLT films. This situation occurs because the index of refraction of the materials actually represents the dielectric constant at optical range and $n = \varepsilon_r^{1/2}$. Therefore, the low-frequency (~ 1 MHz) and high-frequency ($\sim 7.5 \times 10^3$ GHz) response of the PLT films are represented in Figs 7 and 9, respectively. The same compositional dependence of n and ε_r is consequently expected.

3.3. Effect of the substrate

The effect of the substrates used for studying the dynamic response of the PLT thin film to step signals, is shown in Fig. 10. The films deposited on bare silicon or buffer layer ($SrTiO_3$)-coated silicon both exhibit a typical charging behaviour. Large charge–discharge signals are observed for a forward bias situation and small charge–discharge signals are obtained for a reverse bias situation. This phenomenon again arises as a result of the large depletion region which occurred on the interface in the latter situation. The dynamic response of films coated on a $SrTiO_3$/Si substrate was significantly larger than that deposited on a bare silicon substrate.

Both the 550 and 600 °C annealed films are of perovskite structure, as revealed by the X-ray diffraction patterns shown in Fig. 3e and f. No second phase

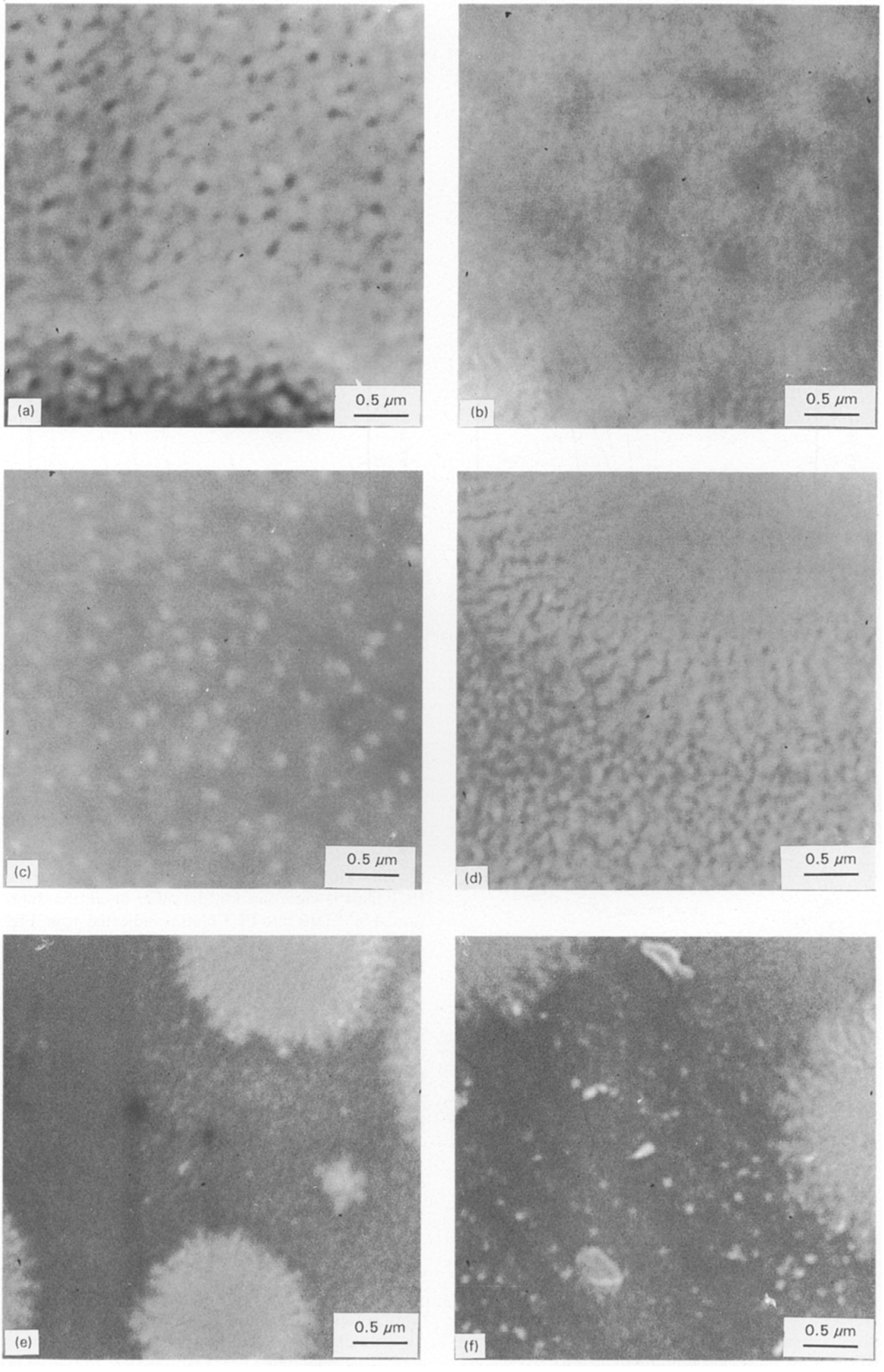

Figure 5 Micrographs of 600 °C annealed films of (a) $PbTiO_3$, (b) PLT 5, (c) PLT 10, (d) PLT 15, (e) PLT 20, (f) PLT 25.

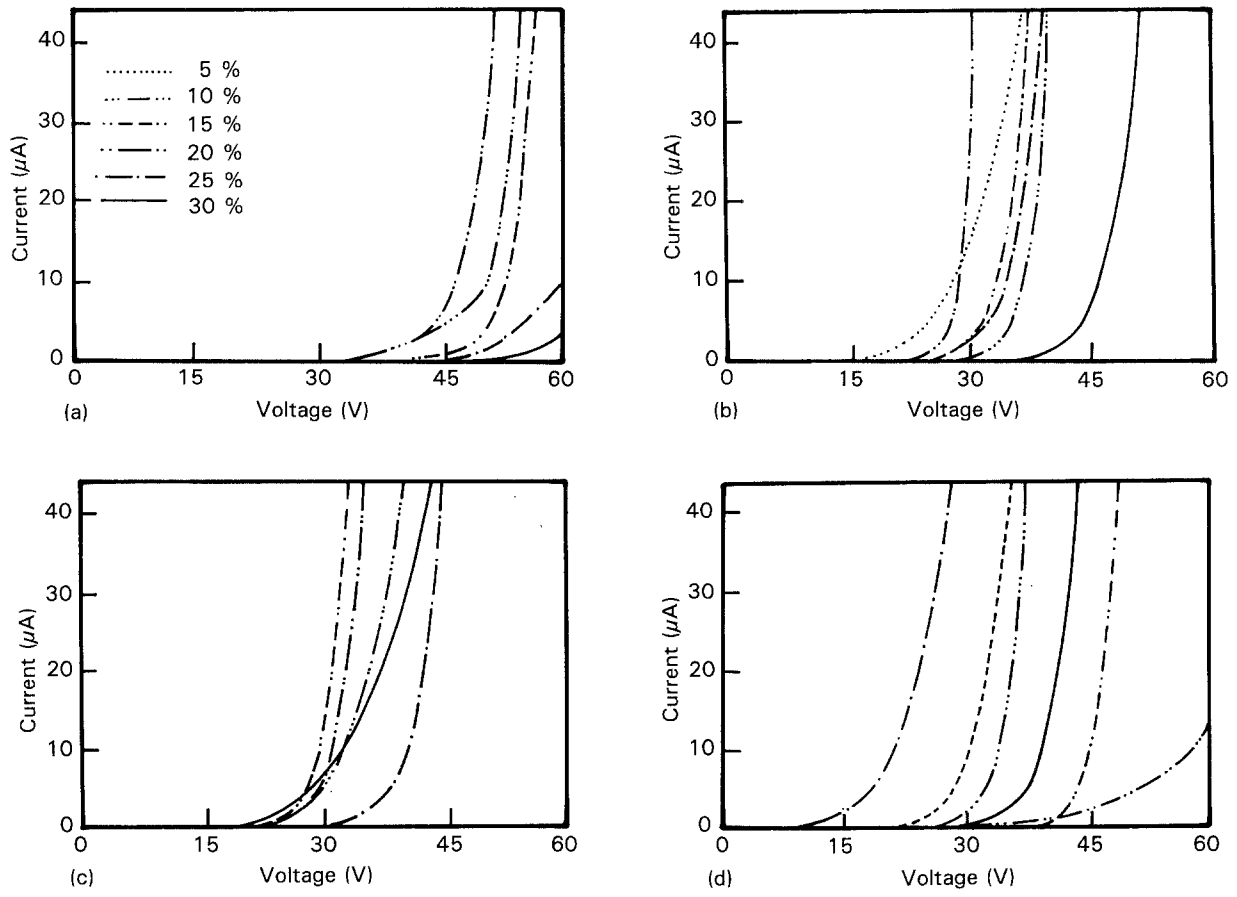

Figure 6 Current–voltage characteristics of PLT films annealed at (a) 550 °C, (b) 600 °C, (c) 650 °C and (d) 700 °C.

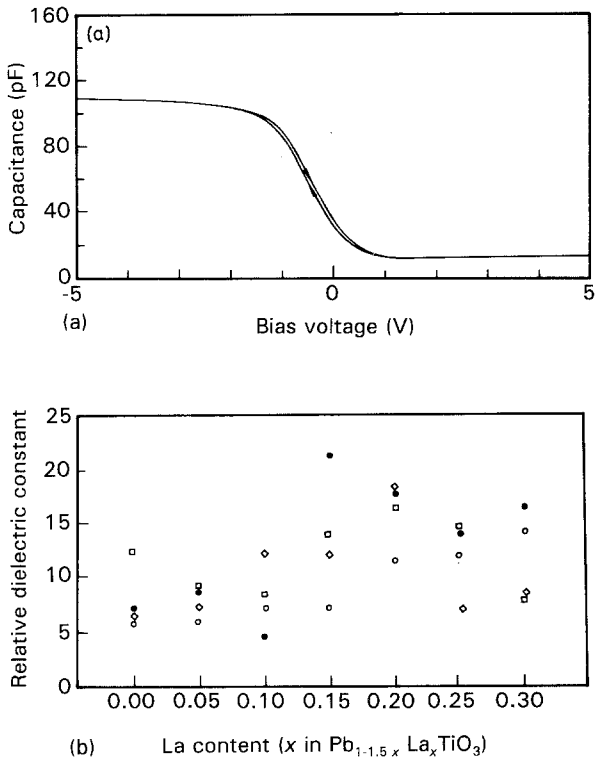

Figure 7 (a) Typical $C-V$ properties (represented by PLT 10), and (b) compositional dependence of dielectric constant of PLT films derived from the $C-V$ curves. (◇) 550 °C, (□) 600 °C, (●) 650 °C, (○) 700 °C.

is observed. The mechanism which produces these films is significantly different from that of bare silicon which, apparently, has nothing to do with the crystallinity of the films.

For the sake of investigating the cause which produced such a behaviour, the compositional profiles of the films deposited on both the substrates were examined using a secondary ion mass spectrometer (SIMS). The interaction between substrate materials and the PLT films is indicated by the results shown in Fig. 11. No constituent of the PLT films, i.e. Pb^{2+}, La^{3+} and Ti^{4+}, is observed from Fig. 11a to be situated beneath the films. Contrarily, the diffusion of Si^{4+} ions into the PLT films is vigorous. On the other hand, the diffusion of Si^{4+} ions into PLT films is indicated, from Fig. 11b, to have become completely inhibited by the presence of the $SrTiO_3$ buffer layer.

The SIMS profiles clearly imply that the mechanism by which the substrate materials influences the electrical properties of the PLT films is a consequence of the interface interactions. The PLT films on bare silicon contain significant amounts of Si^{4+} ions, which are probably in the form of amorphous silica, such that the dielectric properties become tremendously lowered. On the other hand, the films deposited on $SrTiO_3$/Si substrate demonstrate a remarkable charge storage capacity owing to the blocking of Si^{4+} ions by the $SrTiO_3$ buffer layer.

4. Discussion

The phenomenon whereby an amorphous form of the films possesses a lower leakage current density than the crystalline films, has also been observed in other perovskite materials [12]. One possible explanation would be that the grain boundaries formed in the

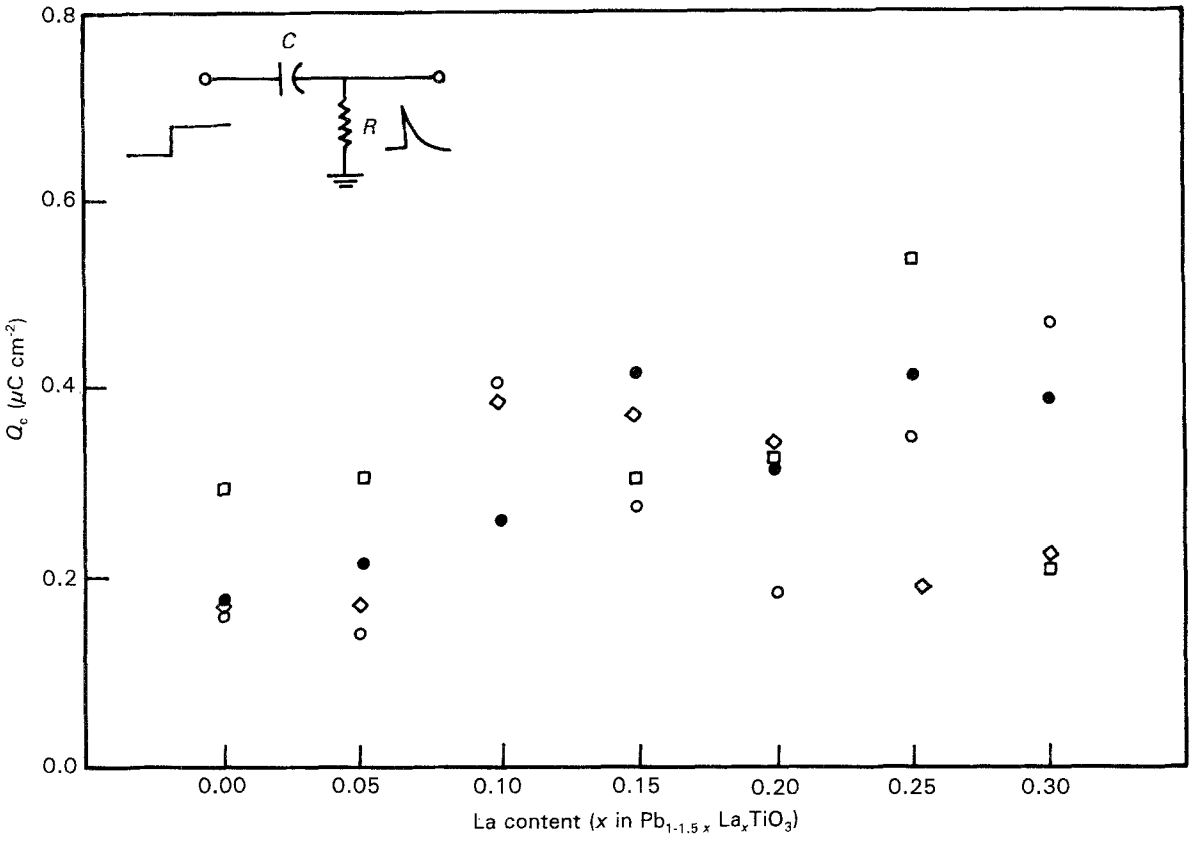

Figure 8 Compositional dependence of charge storage density of PLT films derived from I–T curves. (◇) 550 °C, (□) 600 °C, (●) 650 °C, (○) 700 °C.

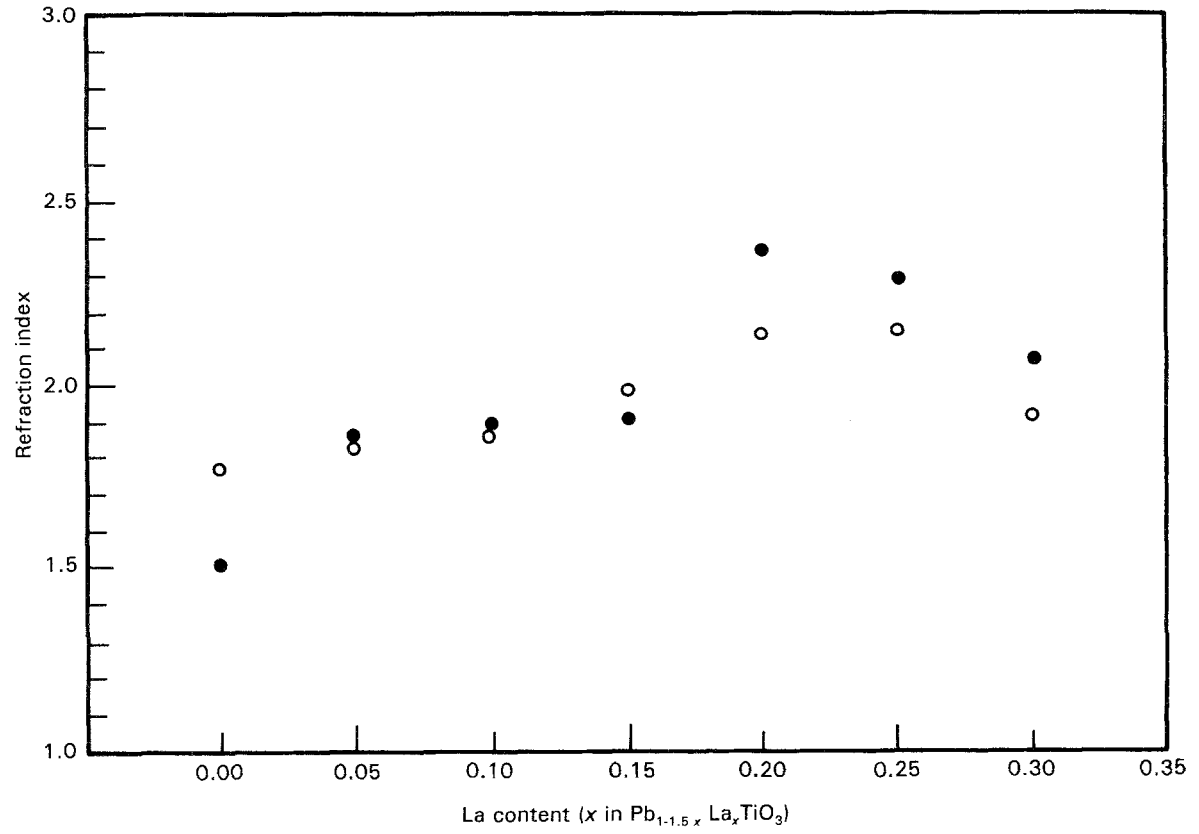

Figure 9 Compositional dependence of index of refraction of PLT films. (○) 600 °C, (●) 650 °C.

polycrystalline film provide a low-resistance path for electrical conduction such that the breakdown has occurred at a much lower voltage. Another factor, however, arises e.g. the point defect induced, which might also possibly contribute towards this phenomenon. This factor is briefly discussed below.

The PLT materials, one of the family of perovskite ceramics with the crystal structure shown in Fig. 12a,

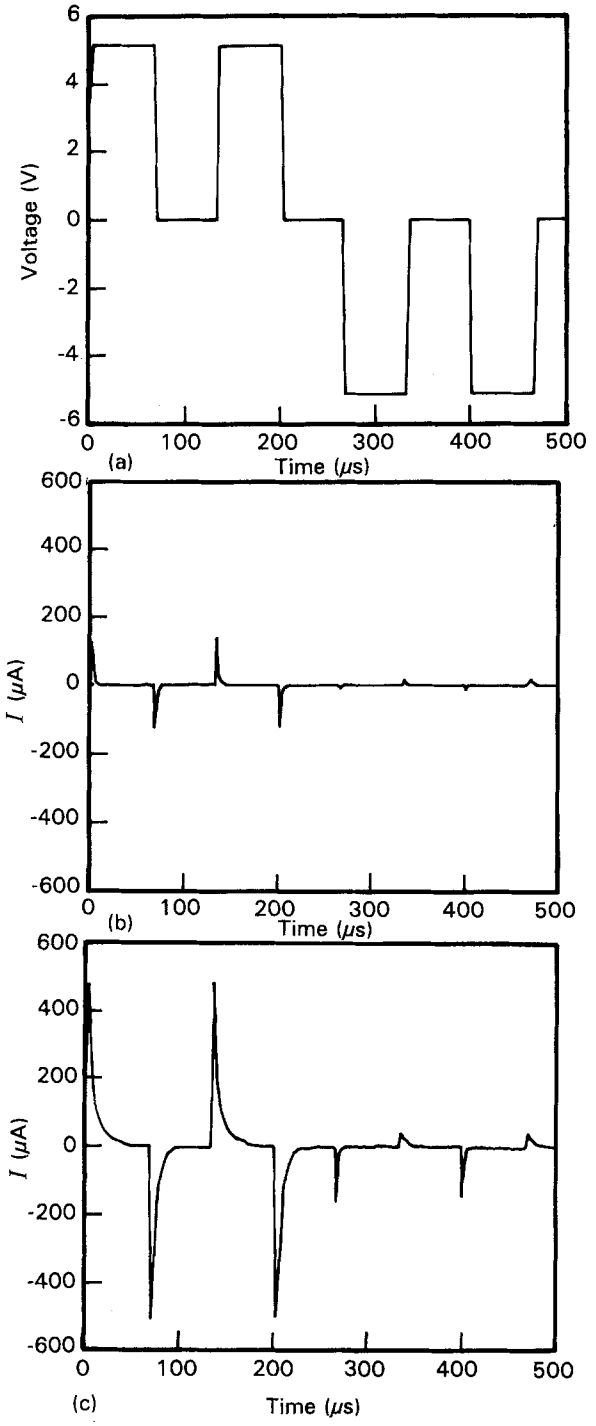

Figure 10 (a) The testing signals, and charging–discharging characteristics of PLT films coated on (b) bare silicon and (c) $SrTiO_3$-coated silicon.

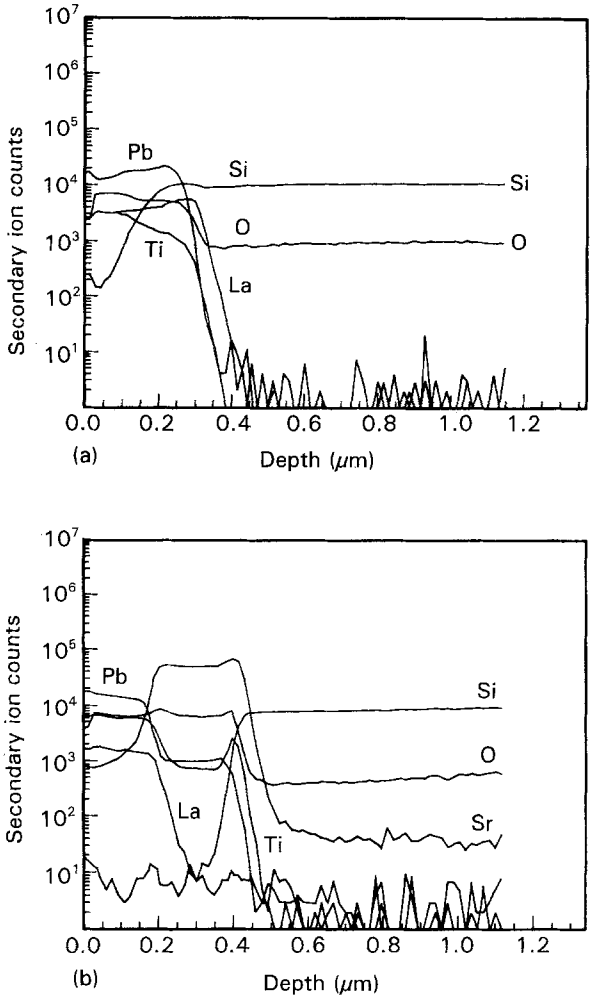

Figure 11 The depth profile of the composition of PLT films coated on (a) bare silicon, and (b) $SrTiO_3$-coated silicon.

can also be viewed in Fig. 12b as being constructed with corner-shared $(TiO_6)^-$ octahedra. The titanium cations are situated at the centre of the octahedra (O site); while the lead and lanthanum cations are distributed at interstitial sites surrounded by eight octahedra, i.e. dodecahedral sites (D site). All of the dodecahedral sites are occupied by Pb^{2+} ions in $PbTiO_3$ materials and some of these sites are observed in Fig. 12b to be occupied by La^{3+} in $Pb_{(1-1.5x)}La_xTiO_3$ materials. In the latter case, vacancies are generated in order to compensate for the extra positive charge of the La^{3+} ions being incorporated. The cationic vacancies concentration required is proportional to the amount of lanthanum ions being added. Restated more precisely, the PLT materials should be formulated as $Pb_{(1-1.5x)}La_x\square_{0.5x}TiO_3$. The vacancies have been assumed to be preferentially induced at A-sites of perovskite due to the fact that PbO is more volatile and Pb^{2+} ions are located at loosely bound dodecahedral sites; while the TiO_2 are non-volatile and Ti^{4+} ions are located at closely bound octahedral sites. The fact that cationic vacancies easily become induced in the lead-containing perovskite as a result of the high volatility of PbO, is generally true, and has been observed in other lead-containing perovskite ceramics, e.g. PZT, PLZT and PMN ceramics. Once generated, these cation vacancies in perovskite crystals act as acceptors in the ionic crystals which would consequently, significantly lower the insulating resistance of the materials.

The amorphous materials, on the other hand, are also composed of $(TiO_6)^-$ octahedra, but are randomly connected. The interstitial sites in these materials are illustrated in Fig. 12c occasionally to become surrounded by more than eight octahedra. The size of the distorted dodecahedra in amorphous materials is larger than the dodecahedral sites in perovskite structure. More than one Pb^{2+} cation can possibly be fit into those large interstitial sites such that more A-site cations than the number of octahedra can be accommodated in the amorphous materials. The loss of Pb^{2+} ions would not result in the formation of vacancies because these Pb^{2+} ions are compensated for by

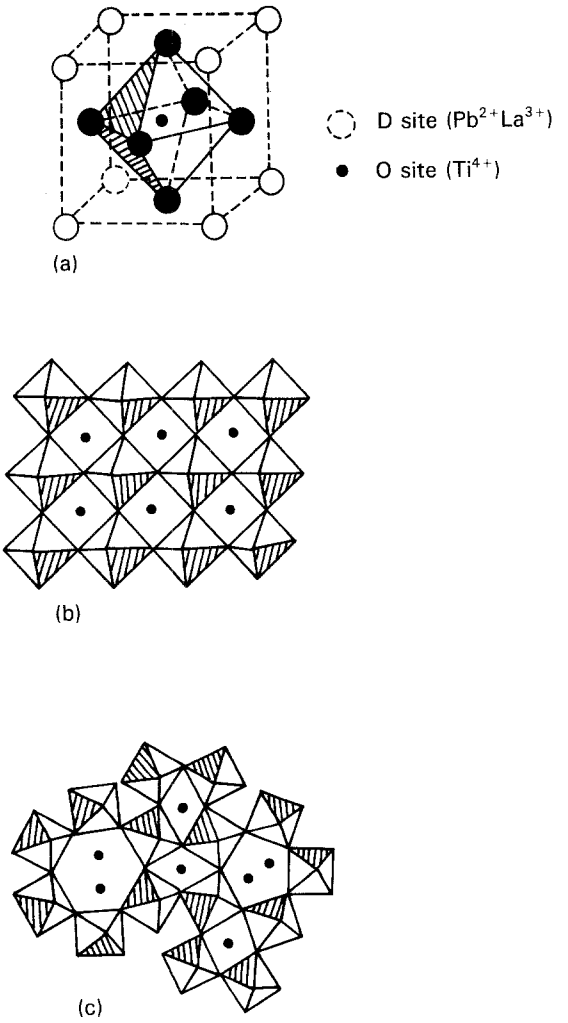

Figure 12 The crystalline structure of $PbTiO_3$ materials: (a) perovskite, (b) corner-shared TiO_6^- octahedron and amorphous structure of $PbTiO_3$ materials, (c) randomly connected TiO_6^- octahedron.

an addition of 5 mol % PbO in the initial composition. In other words, the generation of Pb^{2+} vacancies is entirely prevented in amorphous materials. On the other hand, the objective of suppressing the formation of Pb^{2+} vacancies in crystalline materials by adding excess PbO in the initial materials remains unsuccessful. This is the result of the excess PbO becoming expelled to the grain boundaries whenever the materials crystallize and, consequently, it results in a microstructure consisting of lead-excess grain-boundary phases which surround the stoichiometric grains with $A^{2+}:Ti^{4+}:O^{2-} = 1:1:3$, where A^{2+} is Pb^{2+}, La^{3+} or charge-compensating A-site vacancies. A possibility therefore arises for Pb^{2+} ions to escape from the grain interior, leaving behind low-resistive grains as a result of the formation of excess Pb^{2+} vacancies. The excess Pb^{2+} ions contained in the grain boundaries which surround the grains, would not completely suppress the formation of Pb^{2+} vacancies. The amorphous films are, therefore, comparatively more resistive than the crystalline films, with the breakdown voltage generally also being larger.

All the PLT films exhibit similar dielectric properties, no matter whether they are of amorphous or of perovskite structure. By contrast, the breakdown voltage of amorphous films is significantly higher than that of crystalline films. The discrepancy between dielectric and I–V properties might possibly arise from the fact that the polarization mechanism of PLT materials is different from their conduction mechanism. The unique characteristics of perovskite structure which result in the ferroelectric behaviour of these materials is the spontaneous polarization, which is a result of the off-centred position of Ti^{4+} cations in the octahedra. The octahedra become equilateral once the cubic-to-tetragonal transformation is suppressed. The distribution of the octahedra is uniform in the films because the grains are randomly oriented in polycrystalline films. On the other hand, the $(TiO_6)^-$ octahedra are naturally distributed in a random orientation in the amorphous films. The contribution of induced polarization due to displacement of Ti^{4+} cations inside the octahedra is, consequently, the same small value, whether the films are of amorphous form or crystalline form.

The applicability of the spin-coated PLT series thin films as ferroelectric materials is inferred from the above arguments to be limited. The sol–gel derived films are produced in the amorphous form and the annealing process can only convert the films into crystalline form via the nucleation and growth mechanism. The polycrystalline structure is thus naturally formed, unless some special technique has been applied. Moreover, an abundance of nucleation sites due to the unmatched lattice parameters of perovskite materials and the silicon substrate, will potentially result in ultrafine grains. This kind of microstructure completely suppresses the cubic to tetragonal transformation caused by both the surface energy and constraints exerted by the substrate. Circumventing such a problem would involve future effort placing an emphasis on either synthesizing a highly (0 0 1) texture PLT film or else utilizing ferroelectric films of nearly cubic structure, e.g. rhombohedral PZT, PLZT, etc. Both routes are being developed in our laboratories.

5. Conclusion

The $Pb_{(1-1.5x)}La_xTiO_3$ thin films have been synthesized in the present work using the sol–gel spin-coating technique. The films are around 0.3 μm thick and become completely crystallized once the spin-coated films are annealed at 600 °C and higher temperature. The breakdown voltage is around 30 V for 600–650 °C annealed films and varies only slightly with composition. The amorphous films possess a higher breakdown voltage than the crystalline films and this breakdown voltage is possibly caused by the suppression of lead-vacancy formation as a result of the 5 mol % excess lead included.

Both the amorphous and crystalline films possess similar ferroelectric properties. The dielectric constant, charge storage density and optical index of refraction of the films are $\varepsilon_r = 5$–20, $Q_c = 0.12$–$0.54\ \mu Ccm^{-2}$ and $n = 1.6$–2.3, respectively. They increase moderately with La^{3+} content in the films. A possible reason why these properties are not modified as the amorphous films crystallize is that the octahedra are equilateral, whether the films are amorphous or crystalline.

Low electrical properties of PLT films deposited on bare silicon are ascribed to the diffusion of Si^{4+} ions into the films which have reduced the proportion of dielectric materials. The PLT films synthesized on silicon substrates coated with $SrTiO_3$ as a buffer layer, exhibit a high charge storage density.

Acknowledgements

The authors thank National Science Council for financial support under contract NSC81-0404-E007-547, and also Yong-Chien Ling, Professor, for help in obtaining the SIMS profiles.

References

1. K. KUSHIDA and H. TAKEUCHI, *IEEE Trans. Ultra. Ferro. Freq. Control* **38** (1991) 656.
2. R. TAKAYAMA, Y. TOMITA, K. IIJIMA and I. UEDA, *Ferroelectrics* **118** (1991) 325.
3. A. ARIIZUMI, K. KAWAMURA, I. KIKUCHI and I. KATO, *Jp. J. Appl. Phys.* **24** supp. 24-3 (1985) 7.
4. R. W. WEST, *Ferroelectrics* **102** (1990) 53.
5. K. D. BUDD, S. K. DEY and D. A. PAYNE, *Proc. Br. Ceram. Soc.* **36** (1985) 107.
6. S. J. MILNE and S. H. PYKE, *J. Am. Ceram. Soc.* **74** (1991) 1407.
7. C. CHEN and D. F. RYDER Jr, *ibid.* **72** (1989) 1495.
8. Y. SHIMIZU, K. R. UDAYAKUMAR and L. E. CROSS, *ibid.* **74** (1991) 3023.
9. R. W. SCHWARTZ, B. A. TUTTLE, D. H. DOUGHTY, C. E. LAND, D. C. GOODNOW, C. L. HERNANDEZ, T. J. ZENDER and S. L. MARTINEZ, *IEEE Trans. Ultra. Ferro. Freq. Control.* **38** (1991) 677.
10. S. K. DEY and J. J. LEE, *IEEE Trans. Elec. Devices* **139** (1992) 1607.
11. O. YAMAGUCHI, A. NARAI, T. KOMATSU and K. SHIMIZU, *J. Am. Ceram. Soc.* **69** (1986) C-256.
12. I. H. PRATT and S. FIRESTONE, *J. Vac. Sci. Technol.* **8** (1971) 256.

Received 5 May
and accepted 12 August 1993